

A new class of Zn^{II} and Cr^{III} porphyrins incorporated into porous polymer matrices via an atmospheric pressure plasma enhanced CVD to form gas sensing layers†

Cite this: *J. Mater. Chem. A*, 2014, 2, 1560

Philip Heier,^{ab} Nicolas D. Boscher,^{*a} Torsten Bohn,^c Katja Heinze^{*b} and Patrick Choquet^a

Designed Zn^{II} and Cr^{III} porphyrins (Zn^{II}P, Cr^{III}P(Cl)(H₂O)) and conventional Zn^{II}TPP and Cr^{III}TPP(Cl)(H₂O) are immobilized into porous polysiloxane films via chemical vapor deposition enhanced by an atmospheric pressure dielectric barrier discharge. UV/vis spectroscopy and mass spectrometry prove the integrity of the chromophores after the plasma treatment. The optical amine sensing capabilities of the films are investigated spectroscopically on exposure to triethylamine vapors. A series of coatings with different porphyrin loadings indicate influences of the deposition conditions on the growth of the sensing films and hence the device performance. Additionally, the synthesis and characterization of the novel porphyrin complex Cr^{III}P(Cl)(H₂O) is reported.

Received 2nd September 2013
Accepted 24th November 2013

DOI: 10.1039/c3ta13488a

www.rsc.org/MaterialsA

A. Introduction

Porphyrin based and porphyrin containing coatings are widely investigated for dye-sensitized solar cells,^{1–5} photonic and electronic devices^{6–10} and sensing applications.^{11–28} Porphyrins are of special interest for the design of colorimetric sensors as they exhibit intense absorptions within the visible part of the electromagnetic spectrum. Their absorption characteristics can be changed by interaction of different analytes with the porphyrin macrocycle and especially with the metal center of metalloporphyrins.

Applications of porphyrin based colorimetric sensing surfaces range from the detection of explosives^{11,12} and NO₂^{13–15} over volatile organic compounds (VOC) in general^{16–20} to alcohol vapors^{21–23} and volatile amines in particular.^{24–28} The detection of volatile amines is of special interest as they can be used as

freshness indicators for several food categories.^{29–31} Therefore their detection by smart food packages using colorimetric sensor surfaces may lead to simple yet powerful devices for food quality control used by customers and manufacturers.³²

Preparation of porphyrin based sensing layers has been achieved by different techniques including spin-coating,^{22,13} vacuum evaporation,^{13,22} glow-discharge induced sublimation^{21,13} and Langmuir–Blodgett^{33,34} as well as Langmuir–Schaefer³⁵ techniques. An important approach to improve the overall performance of gas sensing devices is to incorporate the sensing molecules into a suitable stable and adherent matrix. The sensing molecules should be well dispersed within the matrix to prevent agglomeration and tightly trapped to enhance the mechanical stability of the device. On the other hand, the matrix needs to be porous to allow diffusion of analytes towards the sensing sites. Porphyrins have been incorporated into different matrices to form composite sensing layers typically by immobilization in polymers and plasticizers^{25,27,36} or sol-gel deposited silica films.^{12,20,24}

A new arising technology for the preparation of smart composite coatings is chemical vapor deposition (CVD) enhanced by an atmospheric pressure dielectric barrier discharge (AP-DBD). It is a versatile method to deposit thin films from a broad range of precursors and on several substrates.^{37,38} Even heat sensitive polymers can be treated as AP-DBD creates cold plasmas.³⁹ During the process only minor amounts of waste or by-products are produced and inexpensive process gases such as nitrogen⁴⁰ or even air⁴¹ can be used. In contrast to the limitations of industrial implementations of low-pressure plasmas and sol-gel methods, AP-DBD based processes

^aScience and Analysis of Materials Department, Centre de Recherche Public – Gabriel Lippmann, 41 rue du Brill, Belvaux L-4422, Luxembourg. E-mail: nboscher@lippmann.lu

^bInstitute of Inorganic and Analytical Chemistry, Johannes Gutenberg-University Mainz, Duesbergweg 10-14, D-55128 Mainz, Germany. E-mail: katja.heinze@uni-mainz.de

^cEnvironment and Agro-Biotechnologies Department, Centre de Recherche Public – Gabriel Lippmann, 41 rue du Brill, Belvaux L-4422, Luxembourg

† Electronic supplementary information (ESI) available: Molecular structures of $\alpha\alpha$ - and $\alpha\beta$ -H₂P (Fig. S1), UV/vis spectra of Cr^{III}P(Cl)(H₂O) in CH₂Cl₂ pure and with NEt₃ (Fig. S2), IR spectra of Cr-1, Cr-2 and Cr-3 (Fig. S3), UV/vis spectra of Zn-1 under dry and humid conditions with and without NEt₃ (Fig. S4), UV/vis spectra of Cr-3 under dry and humid conditions with and without NEt₃ (Fig. S5), and SEM pictures of Cr-1, Cr-2 and Cr-3 (Fig. S6). See DOI: 10.1039/c3ta13488a

can be easily integrated into roll-to-roll production lines and are indeed already used in industry for thin film deposition, surface cleaning, sterilizing as well as wettability and adhesion enhancement.⁴²

Deposition of lanthanide-containing polymer particles along with siloxane precursors by an AP-DBD method lead to luminescent composite coatings⁴³ while the incorporation of AlCeO₃ nanoparticles in a similar matrix gave rise to anti-corrosive layers.⁴⁴ Bio-active coatings could be achieved by immobilizing enzymes in AP-DBD polymerized acetylene and pyrrole matrices.⁴⁵ The enzymes are reported to be protected from plasma alteration by a surrounding water shell, yet helium has to be used as a process gas.

Recently, the successful incorporation of metallo *meso*-tetraphenylporphyrins (M = Zn^{II}, Cr^{III}) into plasma polymerized siloxane matrices has been achieved.^{46,47} The porosity of the matrices could be controlled by tuning the deposition parameters and first demonstrations of amine sensing properties of these composite coatings have been shown.^{46,48} In this context, novel porphyrins have been developed to improve the optical response upon interaction with amines and to enhance their solubility in the matrix precursor in order to achieve highly colored coatings.⁴⁹ Based on these developments, we herein report the co-deposition of these sophisticated metalloporphyrins Zn^{II}P and Cr^{III}P(Cl)(H₂O) along with siloxane precursors in an AP-DBD enhanced chemical vapor deposition onto aluminum and polyethylene terephthalate (PET) substrates. The integrity of the porphyrin based sensor molecules in the siloxane matrix is investigated by UV/vis spectroscopy as well as by mass spectrometry, while the chemical composition of the hybrid coatings is analyzed by IR and XPS spectroscopy. The gas sensing capabilities of the novel layers are spectroscopically investigated by exposing them to NEt₃ vapors. To rationalize the performances of these coatings, comparable layers containing the *meso*-tetraphenylporphyrins Zn^{II}TPP and Cr^{III}TPP(Cl)(H₂O) were deposited under similar conditions. The amine sensing performance of the devices is correlated with the porphyrin loading of the foils.

B. Experimental section

General materials

The porphyrins Zn^{II}P⁴⁹ and Cr^{III}TPP(Cl)(H₂O)⁵⁰ have been synthesized according to literature procedures and their physical properties agree with reported data. Zinc 5,10,15,20-tetraphenylporphyrin (Zn^{II}TPP), hexamethyldisiloxane (HMDSO, 98.5%), vinyltrimethoxysilane (VTMOS, 98%), dichloromethane (DCM, 99.8%) and triethylamine (NEt₃, 99%) have been obtained from Sigma-Aldrich (St. Louis, MO) and were used without further purification. Nitrogen (99.999%, Air Liquide, Pétange, Luxembourg) was moisturized by bubbling through 18 MΩ water (Millipore, Billerica, MA). Polyethylene terephthalate foil (50 μm thick) has been received from Goodfellow (Huntington, UK) and cold-rolled aluminum foil (200 μm thick, 8011 series) from Eurofoil (Belvaux, Luxembourg).

Synthesis of Cr^{III}P(Cl)(H₂O)

A mixture of $\alpha\alpha/\alpha\beta$ -H₂P metal-free porphyrins (see Fig. S1†) has been synthesized according to literature procedures.⁴⁹ Under an inert atmosphere a 1 : 1 mixture of $\alpha\alpha/\alpha\beta$ -H₂P isomers (300 mg, 0.33 mmol, 1.0 eq.) and Cr(CO)₆ (1.47 g, 6.67 mmol, 20 eq.) have been dissolved in dry and degassed toluene (175 mL) and the mixture was heated to reflux for 24 h. The Cr(CO)₆, which has sublimated on the top of the flask during this time, was transferred back into the solution several times. The reaction mixture was cooled to room temperature (RT) and 0.5 mL of concentrated aqueous HCl was added. After stirring at RT under air for 2 h, the solvents have been removed *via* distillation and residual Cr(CO)₆ *via* sublimation. The obtained dark solid was dissolved in CHCl₃ (75 mL) and filtered. The filtrate was purified *via* column chromatography on Al₂O₃ (Brockmann activity IV, CHCl₃). The first fraction containing metal free $\alpha\alpha/\alpha\beta$ -H₂P has been discarded while the second collected fraction contained the purified product. After removing the solvent under reduced pressure, 231 mg (0.23 mmol, 70%) of Cr^{III}P(Cl)(H₂O) was isolated as a purple solid.

UV/vis (CH₂Cl₂): λ_{\max} (ϵ) = 282 (7.2×10^4), 290 (6.7×10^4), 300 (6.6×10^4), 322 (3.6×10^4), 337 (3.2×10^4), 363 (2.8×10^4), 398 (4.17×10^4), 452 (26.4×10^4), 565 (1.16×10^4), 602 ($0.63 \times 10^4 \text{ M}^{-1} \text{ cm}^{-1}$) nm. MS (ESI⁺): m/z = 948.33 [M - Cl - H₂O]⁺, 966.34 [M - Cl]⁺, 989.33 [M - Cl + Na]⁺, 1005.30 [M - Cl + K]⁺. HR-MS (ESI⁺): m/z = 948.3282 (calcd for C₆₆H₄₈CrN₄: 948.3284).

Plasma deposition

The general procedure employed to create the composite coatings *via* an AP-DBD enhanced CVD has been described before, including the schematic setup of the prototype.^{43,47} The coatings described here vary in the type of the porphyrin and the porphyrin concentration within the precursor solutions, while all other deposition parameters were kept constant.

With help of an ultrasonic atomizing nozzle (Sono-Tek Corporation, Milton, NY) operating at 48 kHz and fed by a syringe driver delivering 0.25 mL min⁻¹ the precursor solution was sprayed onto the respective substrate (PET foil, 50 μm thick; aluminum foil, 200 μm thick), which was placed on the aluminum moving stage of the AP-DBD reactor. The moving stage speed, set up to 6 m min⁻¹, allowed prompt exposition of the formed liquid layer to the plasma discharge in order to polymerize the siloxane precursor. The delay time between the liquid layer deposition and the plasma treatment was one second. The AP-DBD reactor consisted of two flat parallel high voltage electrodes (0.7 × 13 cm²) covered with alumina and the moving stage as the grounded electrode. The discharge gap between the high voltage electrode and the substrate placed on the grounded electrode was maintained at 1 mm. The AP-DBD reactor was fed by a 20 L min⁻¹ nitrogen flow containing 200 ppm HMDSO vapor. The plasma discharge was ignited by means of a 10 kHz sinusoidal signal, chopped by a 1667 Hz rectangular signal. The operating discharge power density was maintained at 0.5 W cm⁻². 100 passes were performed, corresponding to 14 s effective deposition time.

Coatings on PET foils were used for UV/vis studies, amine sensing experiments, XPS analysis and top view SEM. Coatings on aluminum foils were used for IR measurements.

Characterization of deposited layers

Scanning electron microscopy (SEM) was performed on a Hitachi SU-70 FE-SEM. Prior to SEM observations the non-conductive samples were sputter coated with a thin layer of platinum to prevent charging. FT-IR analysis was performed on a Bruker Hyperion 2000 spectrometer equipped with a Ge-ATR-crystal. XPS analyses were realized with a Kratos Axis-Ultra DLD instrument using a monochromatic Al K_{α} X-ray source ($h\nu = 1486.6$ eV) at a pass energy of 20 eV. Extracts of the deposited layers were obtained by rinsing the foils repetitively with 10 mL of ethanol. The collected extracts were concentrated prior to analysis. The HPLC-MS analysis of the Zn-1 extracts were performed on a Dionex Ultimate 3000 HPLC system coupled with an AB/Sciex API 3200 triple-quadrupole tandem MS. The analytical column was an Agilent Zorbay Bonus-RP (150 mm \times 4.6 mm \times 5 μ m). The eluents were H_2O and acetonitrile, both containing 0.1% formic acid. The gradient profile started with 50% acetonitrile during 2 min, then the acetonitrile fraction was increased to 100% over 3 min and then kept at 100% for 7 min. The flow rate was kept constant at 1 mL min^{-1} and the column temperature was 40 $^{\circ}C$. The mass spectrometer was operated in positive electrospray ionization mode and detection was done in full-scan mode. The high-resolution mass spectra of the Cr-1 extracts were collected using a LTQ-Orbitrap Elite hybrid mass spectrometer (ThermoFisher Scientific) equipped with an electrospray ionization source (ESI). The liquid samples were injected by loop injection in a constant flow of methanol. No separation step by liquid chromatography was performed before analysis. The averaged mass spectra were collected in full scan mode at high resolution, allowing a relative error of the measured m/z ratio below 2 ppm.

Amine sensing experiments

The gas sensing properties of the deposited coatings were tested at 20 $^{\circ}C$ by a DU800 Beckman Coulter UV/vis spectrometer with a home-build gas flow setup, which has been described in detail elsewhere.⁴⁸ The foils were placed in 3 mL septum capped quartz cuvettes through which a constant gas flow of 250 mL min^{-1} was passed. Prior to amine exposure, the cuvette was purged with the carrier gas, nitrogen with 50% RH, to monitor the baseline response of the sensing foils and after 10 min the carrier gas was enriched with 1 vol.% NET_3 . The change of the absorption was monitored over 120 min in intervals of 10 s at the specific wavelength at which the foils show the largest change before and after exposure to the amine. These monitoring wavelengths are 434 nm for Zn-1, 428 nm for ZnTPP-1, 446 nm for Cr-1, Cr-2, Cr-3 and 441 nm for CrTPP-1, CrTPP-2 and CrTPP-3. Baseline absorbance was monitored at 500 nm for every data point. Additionally, absorption spectra of the Soret region have been measured before and after exposure to NET_3 .

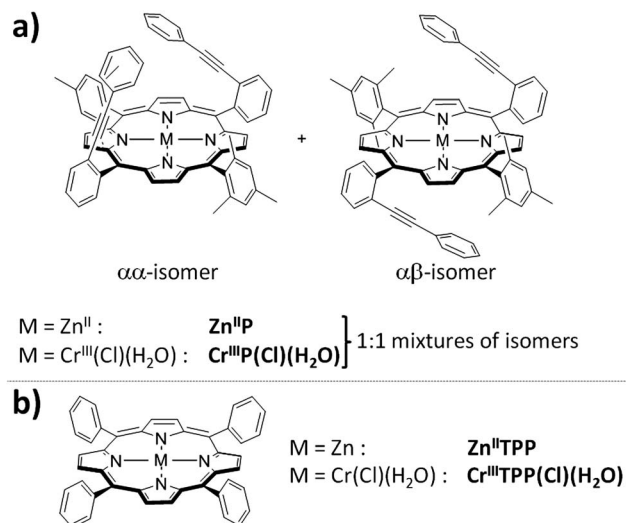


Fig. 1 (a) Molecular structures of the deposited porphyrin complexes $Zn^{II}P$ and $Cr^{III}P(Cl)(H_2O)$ and (b) molecular structures of the deposited reference compounds $Zn^{II}TPP$ and $Cr^{III}TPP(Cl)(H_2O)$.

C. Plasma deposition of sensor coatings

Four different metalloporphyrins were incorporated into porous siloxane matrices *via* AP-DBD enhanced CVD to form colored, transparent and adherent sensing films. The porphyrin complexes $Zn^{II}P$ and $Cr^{III}P(Cl)(H_2O)$ shown in Fig. 1a have been tailored for colorimetric amine sensing by introduction of two phenylalkynyl arms shielding the coordination site.⁴⁹ Both metalloporphyrins were used as a 1 : 1 mixture of $\alpha\alpha$ - and $\alpha\beta$ -isomers. For comparison, the corresponding 5,10,15,20-tetraphenylporphyrins $Zn^{II}TPP$ and $Cr^{III}TPP(Cl)(H_2O)$ (Fig. 1b) were deposited by the same technique and similar process parameters. Table 1 summarizes the compositions of the precursor solutions, which differ in the type and concentration of the porphyrins. All solutions were based on 20 vol.% dichloromethane (DCM) and 80 vol.% vinyltrimethoxysilane (VTMOS), as a siloxane precursor, and contained 0.08 to 3.0 g L^{-1} of the respective porphyrin. The plasma process gas was enriched with hexamethyldisiloxane (HMDSO) vapors, which also contribute to the growth of the porous siloxane matrix in

Table 1 Compositions of the precursor solutions

Porphyrin	Concentration ^a [g L^{-1}]	Foil sample
$Zn^{II}P$	0.75	Zn-1
$Zn^{II}TPP$	0.75	ZnTPP-1
$Cr^{III}P(Cl)(H_2O)$	0.75	Cr-1
	1.50	Cr-2
	3.00	Cr-3
$Cr^{III}TPP(Cl)(H_2O)$	0.75	CrTPP-1 ^b
	0.32	CrTPP-2
	0.08	CrTPP-3

^a In 80 vol.% VTMOS and 20 vol.% DCM. ^b Has been described in ref. 48.

which the porphyrins are incorporated. The general deposition parameters were adapted from the successful process conditions that allowed the deposition of the reference foil CrTPP-1, which has been proven to show the best amine sensing properties within a series of Cr^{III}TPP(Cl)(H₂O) containing layers prepared by the same method (for details see Experimental section).⁴⁸

Deposition of Zn^{II} porphyrin containing coatings

For the Zn^{II}P based coating Zn-1 a solution of 0.75 g L⁻¹ of the respective porphyrin in VTMS/DCM has been used as the precursor solution (Table 1). The solution was sprayed onto the PET substrate by an ultrasonic atomizing nozzle and the sample was subsequently exposed to the AP-DBD. To form the final layer, the substrate was passed 100 times through the precursor mist and the atmospheric plasma (see Experimental section for details). The Zn^{II}TPP containing reference ZnTPP-1 has been prepared using 0.75 g L⁻¹ Zn^{II}TPP in the precursor solution employing the same general deposition process.

Both coatings are adherent to the PET substrate foils and are stable towards water. Neither visually noticeable cracks nor particles were observed on the surface by eye. They show similar FT-IR spectra with the characteristic absorptions of plasma-polymerized organosiloxanes (see Fig. 2). The strong and broad band observed at 1087 cm⁻¹ is assigned to a Si-O-Si network vibration while the absorptions at 806 cm⁻¹ ($\nu(\text{Si-CH}_3)$), 847 cm⁻¹ ($\nu(\text{Si-C})$ and $\rho(\text{CH}_3)$), 1261 cm⁻¹ ($\delta^s(\text{Si-CH}_3)$), 1409 cm⁻¹ ($\nu^a(\text{CH}_3)$), 2915 and 2960 cm⁻¹ ($\nu(\text{CH}_3)$) prove the high retention of the methyl groups from the siloxane monomer.⁵¹ The peak observed at 1675 cm⁻¹ is commonly observed for nitrogen plasma-polymerized organosiloxanes and is attributed to C=N vibrations, as nitrogen is partially incorporated from the plasma

gas.⁴⁰ No distinct vibrations from the incorporated porphyrin macrocycles can be observed, as they are hidden by the intense matrix vibrations. XPS analysis shows an elemental composition as expected for carbon rich plasma-polymerized organosiloxanes due to high methyl group retention. Zn-1 is composed of 16 at.% silicon, 25 at.% oxygen, 55 at.% carbon and 4 at.% nitrogen, while for ZnTPP-1 16 at.% silicon, 26 at.% oxygen, 54 at.% carbon and 4 at.% nitrogen are observed. This is in good agreement with literature values.^{46,47} As the zinc content of the incorporated porphyrins is rather low (0.84 at.% in Zn^{II}P and 1.3 at.% in Zn^{II}TPP) only traces of zinc could be detected by XPS in the foil. The deposited matrix Zn-1 contains (0.2 ± 0.1) at.% zinc and ZnTPP-1 (0.3 ± 0.1) at.%, which represents a relatively high porphyrin loading of the matrix of about (22 ± 8)% in both cases.

Both foils show uniform transparent pale orange-green coloration and exhibit the characteristic UV/vis absorption spectra of the incorporated intact metalloporphyrin macrocycle. The foils show Soret band absorptions at 433 nm for Zn-1 (Fig. 3a) and at 428 nm for ZnTPP-1 (Fig. 4a). These absorptions are shifted bathochromically by 14 nm as compared to the spectra observed for Zn^{II}P and Zn^{II}TPP in *n*-hexane solutions. Q-band absorptions are found at 565 and 603 nm and at 560 and 600 nm for Zn-1 and ZnTPP-1, respectively. UV/vis spectra of porphyrins are known to be affected by their environment as emphasized by the solvatochromic series. In solution their absorption is known to be red-shifted in polar solvents.⁴⁹ A similar effect may be responsible for the bathochromic shift within the polysiloxane matrix, as it contains several polar groups. The rigidity of the matrix can additionally lead to a slight distortion of the entrapped porphyrin macrocycles which is also known to induce bathochromic shifts. The red-shift of the porphyrins' absorption within the matrix may therefore be attributed to a general solvatochromic effect. The UV/vis spectra

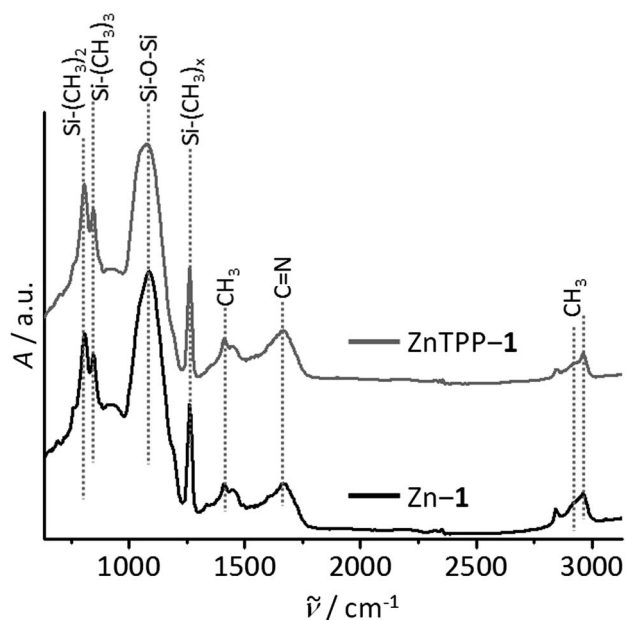


Fig. 2 FT-IR absorption spectra of Zn-1 on aluminum (bottom, black) and ZnTPP-1 on aluminum (top, grey).

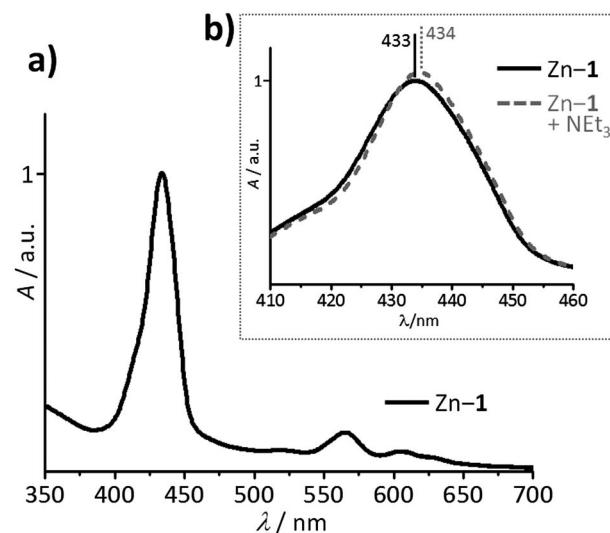


Fig. 3 (a) Normalized UV/vis absorption spectrum of Zn-1 with the Soret band absorption at 433 nm and Q-band absorptions at 565 and 603 nm and (b) magnification of the Soret band region before (black, solid) and after (grey, dotted) 2 h exposure to 1% NEt₃ vapor.

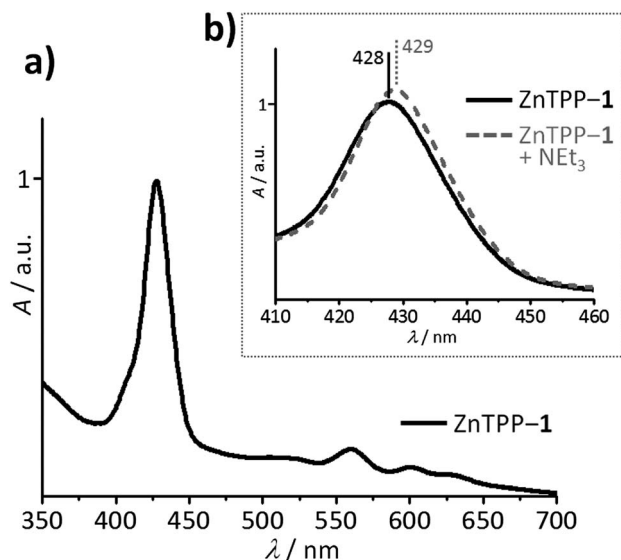


Fig. 4 (a) Normalized UV/vis absorption spectrum of ZnTPP-1 with the Soret band absorption at 428 nm and Q-band absorptions at 560 and 600 nm and (b) magnification of the Soret band region before (black, solid) and after (grey, dotted) 2 h exposure to 1% NEt_3 vapor.

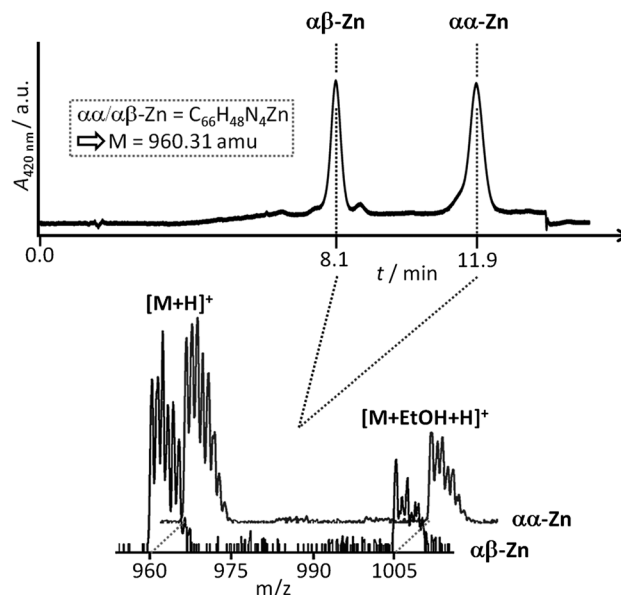


Fig. 5 Top: chromatogram of the HPLC-MS analysis of extracts from Zn-1; bottom: ESI-MS analysis of the respective peaks at 8.1 min (front) and 11.9 min (back).

strongly indicate that the macrocycle is unaltered by the plasma deposition process. As FWHM values of the Soret band are similar to values observed in solution, stacking and aggregation of the porphyrins is obviously suppressed by their thorough and stable dispersion within the matrix.

The integrity of the relatively simple Zn^{II} TPP sensor molecule after the described plasma treatment has already been successfully proven by mass spectrometry of ethanol extracts from the layer.⁴⁷ To prove the preservation of the more complex Zn^{II} P structure after the plasma deposition, ethanol extracts of Zn-1 have been analyzed by HPLC-MS. The only prominent peaks seen in the HPLC chromatogram in Fig. 5 can be clearly assigned to the $\alpha\beta$ -isomer of Zn^{II} P at 8.1 min and to the $\alpha\alpha$ -isomer at 11.9 min based on the mass spectral analysis as well as by comparison with literature retention data.⁴⁹ Hence, the entire molecular structure of the sensor molecules, including the shielding phenylalkynyl arms and the labile bound Zn^{II} , is preserved. Moreover, the initial isomeric ratio of 1 : 1 ($\alpha\alpha$: $\alpha\beta$) is unaltered, showing that both isomers are incorporated in the matrix.

Deposition of Cr^{III} porphyrin containing coatings

Cr^{III} porphyrin complexes are known to have high affinity towards nitrogen containing axial ligands (*e.g.* amines) and they show large spectral changes upon interaction with amines in solution. Therefore, they are good candidates for the preparation of amine sensing devices. We have recently reported the formation of Cr^{III} TPP(Cl)(H_2O) containing layers by AP-DBD which are capable of colorimetric amine sensing.⁴⁸ In this context, we have developed the novel porphyrin complex Cr^{III} P(Cl)(H_2O). Its synthesis is described in the Experimental section. In contrast to the trends observed for zinc porphyrin

complexes,⁴⁹ Cr^{III} P(Cl)(H_2O) does not outclass its simple tetraphenylporphyrin equivalent Cr^{III} TPP(Cl)(H_2O) with respect to spectral shifts upon interaction with NEt_3 in solution. In DCM, both Cr^{III} porphyrin complexes show a large hypsochromic shift upon NEt_3 exposure of about 17 nm of the Soret band. For Cr^{III} P(Cl)(H_2O) a shift from 452 to 435 nm is observed in DCM (see Fig. S2[†]), while Cr^{III} TPP(Cl)(H_2O) shows a shift from 448 to 431 nm. The benefit of the Cr^{III} P(Cl)(H_2O) complexes is their strikingly higher solubility in the precursor solution as compared to Cr^{III} TPP(Cl)(H_2O). The solubility of Cr^{III} TPP(Cl)(H_2O) in VTMS : DCM 80 : 20 is 7.8 mmol L^{-1} while 39.3 mmol L^{-1} of Cr^{III} P(Cl)(H_2O) can be dissolved in the precursor solution. The increased solubility of the Cr^{III} P(Cl)(H_2O) complexes is attributed to their molecular structures with the two arms above one or both sites of the porphyrin macrocycle, which suppresses π - π stacking of the porphyrins.⁴⁹ Therefore, significantly higher complex concentrations in the precursor solutions can be used during the deposition process leading to sensing foils with a more intense coloration as compared to the intensities achievable with Cr^{III} TPP(Cl)(H_2O). This is a crucial step towards simple devices for the inspection of food freshness whose response should be visible by the human eye instead of spectrometers.

As indicated in Table 1, Cr^{III} P(Cl)(H_2O) based coatings were deposited from three different precursor solutions containing 0.75 g L^{-1} (Cr-1), 1.50 g L^{-1} (Cr-2) and 3.00 g L^{-1} (Cr-3). The deposition parameters in all cases were equivalent to the ones used for the reference foil CrTPP-1 (see Experimental section for details).⁴⁸ All three Cr^{III} porphyrin containing coatings are adherent to the PET substrate foils and are stable towards water. Neither visually noticeably cracks nor particles were observed on the surface by eye. As the FT-IR spectra are dominated by the absorptions of the plasma-polymerized

organosiloxane matrix rather than by the different incorporated porphyrins, the FT-IR spectra of all foils are similar among each other and also to the one shown in Fig. 2 for Zn-1. Therefore, no signs of the incorporated Cr^{III} porphyrins are detected in the FT-IR spectra of Cr-1, Cr-2 and Cr-3 (Fig. S3†). The chromium percentage of Cr-1 is expected to be around the 0.2 at.% as that observed for zinc in Zn-1, as deposition parameters and solution concentrations are equal for Zn^{II} and Cr^{III} containing coatings. But in contrast to zinc, chromium contents could not be quantified in foils Cr-1, Cr-2 and Cr-3 reliably down to this range by XPS, as the signals are hardly above the noise level. This is probably because the Relative Sensitivity Factor (RSF) of the Cr 2p is smaller compared to Zn 2p (RSF_{Cr2p} = 2.4; RSF_{Zn2p} = 5.59). The elemental composition estimated by XPS regarding silicon, oxygen, carbon and nitrogen is similar to the one measured for the zinc porphyrins containing coating Zn-1 and ZnTPP-1.

The coloration of the three Cr^{III}P(Cl)(H₂O) containing foils varies from slightly green for Cr-1 to intense green for Cr-3 (see insets in Fig. 6). Their UV/vis absorption spectra show the characteristic absorptions of intact Cr^{III} porphyrin complexes at the same energy for each foil. The absorptions of Cr-1 to Cr-3 only grow in intensity (Fig. 6). Hence even though the different porphyrin loadings within the coatings could not be estimated by XPS, the absorption spectra corroborate that the porphyrin content is proportional to their concentration within the initial precursor solutions. The intense Soret band absorption is seen at 458 nm and the weaker Q-band absorptions at 572 and 612 nm. The weak absorption at 400 nm is characteristic for Cr^{III} porphyrin complexes with anionic axial ligands and is attributed to a $\pi(a_{2u}, a_{1u}) \rightarrow d(e_g)$ charge transfer absorption from the porphyrin to the metal center.⁵² The presence of these UV/vis absorptions is a strong indicator that neither the molecular structure of the porphyrin macrocycle nor the oxidation state of the chromium central metal is changed during the plasma deposition process.

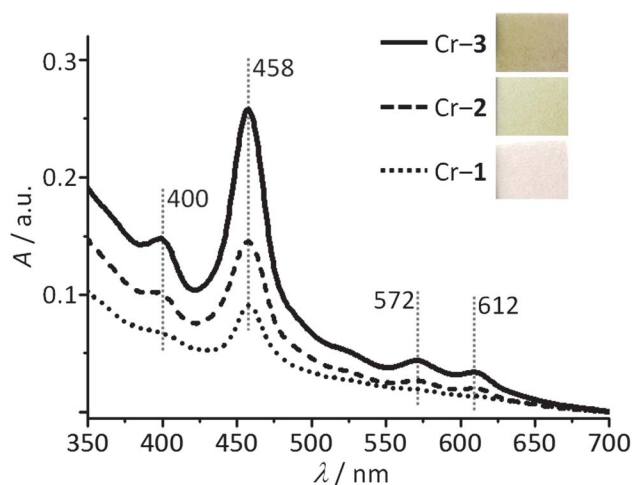


Fig. 6 UV/vis absorption spectra of Cr-1 (dotted), Cr-2 (dashed) and Cr-3 (straight) with a charge transfer absorption at 400 nm, the Soret band absorption at 458 nm and Q-band absorptions at 572 and 612 nm; insets show photographs of the respective foils.

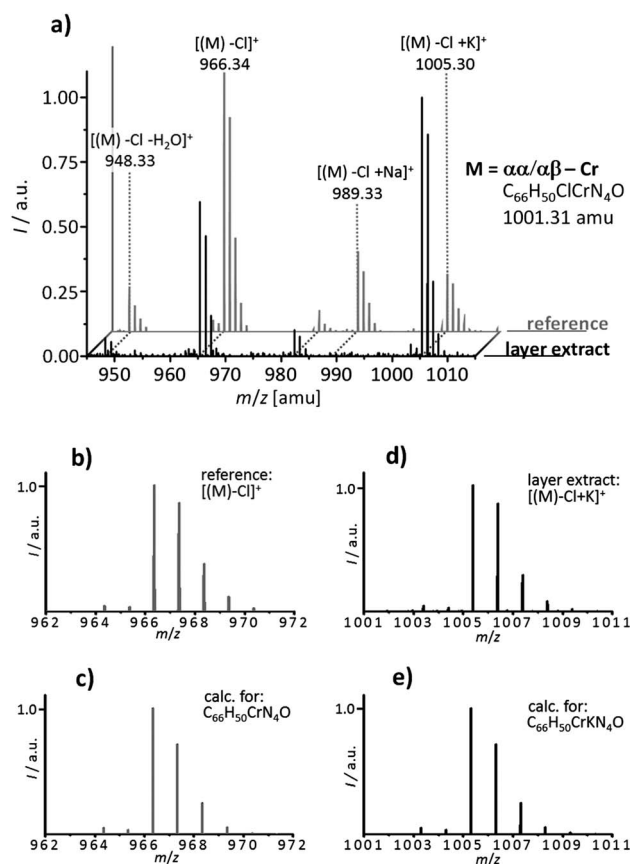


Fig. 7 (a) ESI mass spectrum of extracts from Cr-1 (black, front) and the reference ESI mass spectrum of Cr^{III}P(Cl)(H₂O) before plasma deposition (grey, back); each spectrum is normalized to the most intense peak; (b) and (d) magnification of the most intense peak of the reference spectrum and the layer extract analysis, respectively; (c) and (e) calculated isotopic pattern for [(M) - Cl]⁺ and [(M) - Cl + K]⁺, respectively.

To further substantiate the integrity of the molecular structure during the deposition, ethanol extracts of the coatings were studied by mass spectrometry (for details see Experimental section). As no method could be developed to separate the Cr^{III}P(Cl)(H₂O) isomers *via* HPLC, as was successful for Zn^{II}P,⁴⁹ the samples were analyzed *via* high resolution ESI mass spectrometry. Fig. 7a shows a representative mass spectrum of the Cr-1 extracts in the front (black) and the reference mass spectrum of molecular Cr^{III}P(Cl)(H₂O) before plasma deposition in the back (grey). The spectra clearly demonstrate the integrity of the porphyrin macrocycle, the retention of the shielding phenylalkynyl arms and the presence of the metal in the porphyrin. Experimental isotopic patterns shown in Fig. 7b and d match with calculated patterns (Fig. 7c and e, respectively) revealing the correct assignments of the fragmentation peaks.

D. Amine sensing experiments

To probe the colorimetric amine sensing ability of the deposited coatings, foil samples were placed in a 3 mL flow cuvette and exposed to a constant flow of 1 vol.% NEt₃ vapor in the carrier

gas (N_2 with 50% relative humidity) over 2 h (for details see Experimental section). The initial absorption of the Zn^{II} and Cr^{III} containing foils does not change under humid conditions as compared to the inert atmosphere. The amine sensing performance of zinc porphyrin containing foils is also not affected by change of the relative humidity (RH) in the carrier gas (see Fig. S4†). In contrast, the performance of the chromium porphyrin based matrices is greatly enhanced under humid conditions (see Fig. S5†). For real-life applications like *e.g.* food packaging the compatibility under humid conditions is rather beneficial than detrimental, as the ubiquitous humidity gives no false response with the sensor system but enhances its performance. The detailed mechanism of the interaction of Cr^{III} porphyrins with NEt_3 either in solution or in polymer matrices under different humid conditions is currently under investigation in our laboratories and mechanistic results will be published in due course.

Amine sensing with Zn^{II} porphyrins

The Soret band absorptions of Zn-1 and ZnTPP-1 before (solid line) and after (dotted line) 2 h of exposure to 1 vol.% NEt_3 in the carrier gas are shown in Fig. 3b and 4b, respectively. Zn-1 shows a small 1 nm bathochromic shift of the Soret band from 433 to 434 nm upon interaction with NEt_3 and a slight increase in intensity along with a decrease of the FWHM of the signal. Similar minor changes are observed for ZnTPP-1 with a Soret band shift from 428 to 429 nm. The colorimetric responses of the sensing foils are not as large as the ones reported for the respective porphyrin complexes exposed to NEt_3 in *n*-hexane solutions. Under homogenous conditions, the Soret band of $Zn^{II}TPP$ in *n*-hexane is shifted by 11 nm from 414 to 425 nm and the one of $Zn^{II}P$ by even 13 nm from 419 to 432 nm upon amine coordination.⁴⁹ As intact molecular sensors are embedded within the matrix (see previous section), the observed discrepancy between the sensor's performance in *n*-hexane solution and in the matrix must be attributed to other reasons. One possibility may be a poor accessibility of the chromophores within the matrix. Another issue could be an environmental matrix effect. It has been shown in serial trials with different solvents that the absorption shifts upon NEt_3 coordination decrease as the initial Soret absorption is shifted bathochromically.⁴⁹ For instance in chloroform solutions the bathochromic shift upon interaction with NEt_3 also amounts only to 1 nm from 428 to 429 nm. Therefore, we propose that the diminished absorbance shifts of the sensor molecules entrapped in the matrix is rather ascribed to sensor-matrix interactions, comparable to the solvatochromic effect observed in solution, than indicating a low porosity of the matrix.

Amine sensing with Cr^{III} porphyrins

The foils Cr-1, Cr-2 and Cr-3 were placed in flow cuvettes and exposed to a constant flow of nitrogen (50% RH) enriched with 1 vol.% of NEt_3 . The responses of the foils were monitored by changes of the Soret band absorption by UV/vis spectroscopy (see Experimental section for details). Fig. 8 shows the Soret band absorptions of the foils before (solid line) and after (dotted

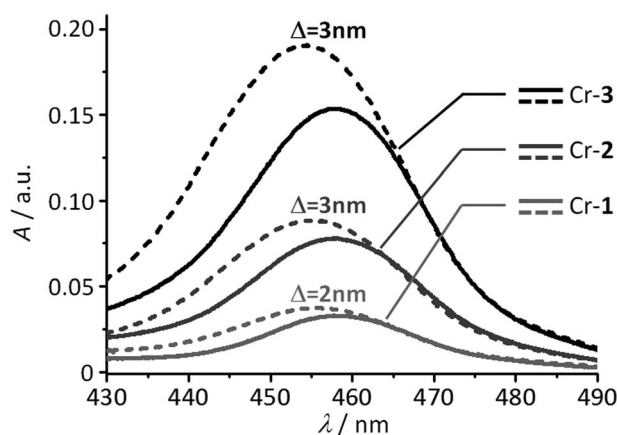


Fig. 8 Soret band UV/vis absorption before (solid lines) and after (dashed lines) 2 h exposure to a constant nitrogen flow containing 1 vol.% NEt_3 for Cr-1, Cr-2 and Cr-3; hypsochromic shifts upon interaction with NEt_3 are indicated above the respective curves.

line) two hours exposure to a nitrogen flow containing NEt_3 . The absorptions are shifted hypsochromically between 2 and 3 nm along with a slight increase in intensity and a broadening of the band (see Table 2). The changes are similar to that of the reference foil CrTPP-1 under identical conditions. The difference spectra of Cr-1, Cr-2 and Cr-3, calculated by subtraction of the spectra before interaction with NEt_3 from the spectra after NEt_3 treatment, are shown in Fig. 9. As already indicated by the different absorptions shown in Fig. 8, the foil with the highest porphyrin loading, Cr-3, gives the largest absolute response upon amine exposure. For all foils the maximum change in absorption is observed at 446 nm.

To measure the dynamic responses of the foils towards amine exposure the changes of the absorptions at 446 nm were monitored referenced to the absorption at 500 nm (baseline) every ten seconds while exposed to a constant flow of 1 vol.% NEt_3 in the carrier gas (N_2 with 50% RH). As the foils have different initial absorption intensities, the recorded responses were normalized to their respective initial Soret band absorption intensity. These normalized absorption changes are depicted in Fig. 10a. During the first 10 min, the foils were exposed to a constant flow of nitrogen with 50% RH without any amine to record the baseline response. The evanescent signals for all foils show that there is no interaction with humidity. After 110 min exposure to a 1 vol.% NEt_3 flow, Cr-1 shows a

Table 2 Compiled UV/vis data for Cr-1, Cr-2 and Cr-3 before and after exposure to NEt_3

Foil sample	As deposited			After NEt_3 exposure ^a		
	Position [nm]	Height [a.u.]	FWHM ^b [nm]	Position [nm]	Height [a.u.]	FWHM ^b [nm]
Cr-1	458	0.03	23.8	456	0.04	27.8
Cr-2	458	0.07	27.5	455	0.09	29.2
Cr-3	458	0.15	28.1	455	0.19	30.6

^a 110 min exposure to 1% NEt_3 . ^b Full width at half maximum.

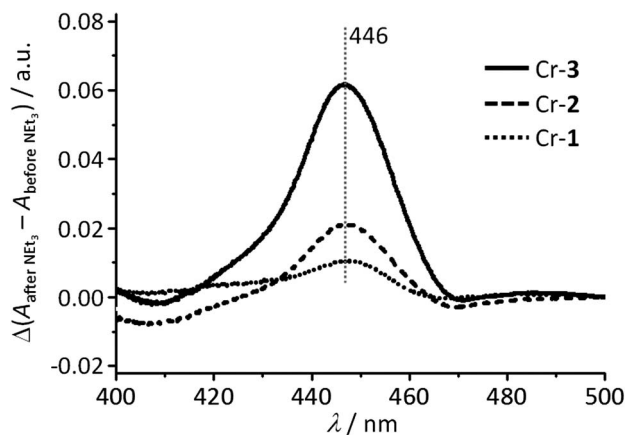


Fig. 9 Difference spectra of Cr-1 (dotted), Cr-2 (dashed) and Cr-3 (solid) calculated by subtraction of the UV/vis spectra before exposure to NEt_3 from the respective spectra after 2 h exposure.

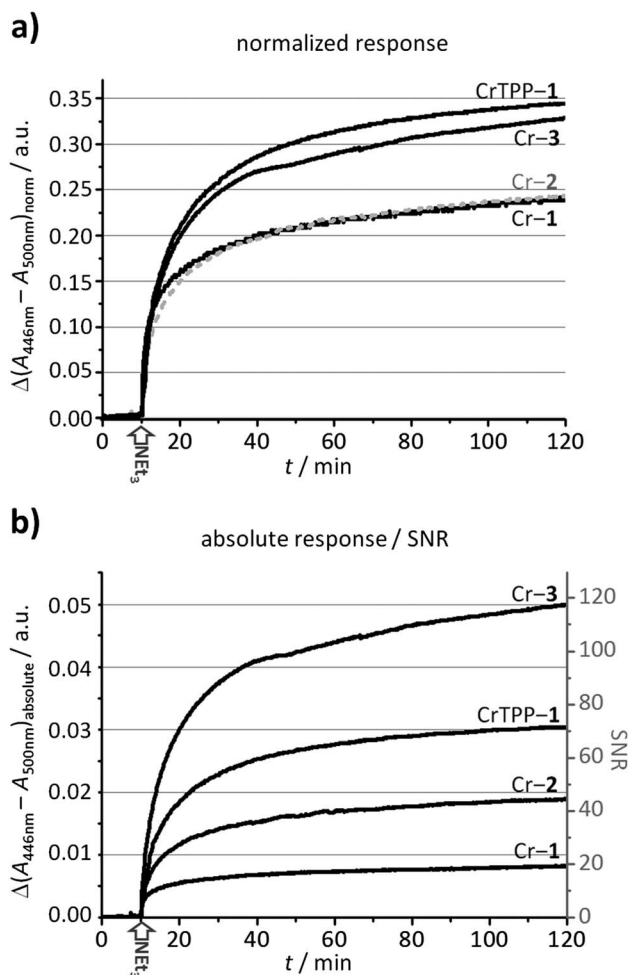


Fig. 10 Time traces of the absorption change at 446 nm relative to the absorption at 500 nm upon exposure to a constant flow of 1 vol.% NEt_3 ; data points measured every 10 s; exposure starts at 10 min; (a) values normalized to the initial Soret band intensity; (b) absolute values as measured by the spectrometer (left scale) and converted to the respective signal-to-noise ratio (SNR, right scale).

normalized response of about 0.25 a.u. This is about one third smaller than that observed with the reference CrTPP-1, which is prepared from the corresponding $\text{Cr}^{\text{III}}\text{TPP}(\text{Cl})(\text{H}_2\text{O})$ containing precursor solution under the same deposition conditions. As the responses are normalized to the initial absorption intensities, this is a sign of less sensor molecules interacting with the analyte in Cr-1 than within CrTPP-1. This difference is also expressed by the absolute responses of the foils and depicted in Fig. 10b. Even though the initial Soret band intensity of the two foils is similar, a significantly smaller signal change is observed for Cr-1 as compared to CrTPP-1.

When the amount of $\text{Cr}^{\text{III}}\text{P}(\text{Cl})(\text{H}_2\text{O})$ is doubled within the sensing layers, the absolute response of the foils towards amine exposure proportionally increases, as can be seen from a comparison of the responses of Cr-1 (0.009 a.u.) and Cr-2 (0.018 a.u.) in Fig. 10b. The normalized responses of Cr-1 and Cr-2, however, are superimposable. The identical normalized responses of Cr-1 and Cr-2 show that the same fraction of sensor molecules interacts with the amines. The similar time profile of the two foils additionally proves that diffusion of the analyte through the matrix is similar. We ascribe this to a similar porosity and similar incorporation of the chromophores accomplished during the deposition process. This indicates that the growth of the matrix and thereby the matrix properties are not significantly affected by doubling the porphyrin concentration within the precursor solution from 0.75 g L^{-1} (Cr-1) to 1.50 g L^{-1} (Cr-2).

This behavior obviously changes when the initial porphyrin concentration is increased to 3.00 g L^{-1} (Cr-3). The normalized response of this foil (see Fig. 10a) is increased as compared to Cr-1 and Cr-2 and is rather similar to that observed for the reference compound CrTPP-1. And even though the initial Soret band intensity is doubled compared to Cr-2 (see Table 2), the absolute response as shown in Fig. 10b is increased by a factor of three. Both illustrations suggest that in Cr-3 a higher fraction of porphyrin molecules interacts with the amines compared to Cr-1 and Cr-2 with lower porphyrin concentrations. This observation indicates that above a certain threshold of porphyrin concentration within the precursor solution, the mechanism of the matrix growth is changed which enables more chromophores to interact with the amine. As can be seen from the normalized response, the fraction of porphyrin sites interacting with the analyte in Cr-1 is comparable to that in CrTPP-1. On the other hand the absolute number of porphyrins within the matrix is higher, which leads to a stronger absolute response of Cr-1. After 110 min exposure to NEt_3 an absolute response of 0.049 a.u. is observed for Cr-1, which represents a 1.6 fold increase as compared to the 0.030 a.u. of CrTPP-1.

To compare the sensors' performance with results from other sensing systems, the foils' responses towards NEt_3 exposure were converted into the respective signal-to-noise ratio (SNR) parameter (see Fig. 10b). This dimensionless value is defined by the observed signal change divided by the signal noise of the chosen analytical method. For a positive detection event, a $\text{SNR} \geq 3$ has been defined.^{12,28} The superior performance of Cr-3 compared to the reference compound CrTPP-1 is also expressed by their SNR values of 117.6 and 70.6,

respectively. This has been achieved by the increased solubility of the novel porphyrin chromophores and hence the higher loading of the foil.

E. Influence of Cr^{III} porphyrin concentration on the sensor properties

As shown in the previous part for Cr-1, Cr-2 and Cr-3, the performance of the deposited layers with respect to colorimetric amine sensing is associated with the porphyrin concentration within the precursor solutions. The normalized responses of the foils as depicted in Fig. 10a show a disproportional dependence on the solution concentrations, with a sudden increase upon a certain threshold. The solubility of the porphyrins in the precursor solution seems to be decisive for this behavior. If the solutions are nearly saturated before deposition, like for Cr-3, small aggregates may be formed upon solvent evaporation during the spray process which may influence the later sensor performance in two ways.

On the one hand, the formed aggregates may act as seeds for the matrix growth leading to a more porous material and therefore enable more chromophores to interact with the amine. Unfortunately, no direct experimental evidence could so far be obtained for this assumption as SEM analyses of the three foils show a similar surface morphology (see Fig. S6†). Cr-1, Cr-2 and Cr-3 do all show smooth surfaces with potential small porosities covered by the platinum layer which has been sputtered onto the samples to avoid charging effects. Attempts to obtain SEM pictures with less or no platinum coating were unsuccessful due to the insulating properties of both the substrate and the layer. On the other hand formation of aggregates during the deposition from nearly saturated solutions may more often lead to spatially close incorporation of the chromophores within a matrix pore. If more than one chromophore is involved in the actual sensing event with NEt₃, this could explain the remarkably higher response of Cr-3.

Even though there is no direct experimental proof for these assumptions, the general dependence of the sensor foils' performances on the initial chromophore concentration in solution becomes obvious by further comparison of the Cr^{III}P(Cl)(H₂O) and Cr^{III}TPP(Cl)(H₂O) systems. As Cr-3 and CrTPP-1 show a similar normalized response towards NEt₃ vapors (Fig. 10a), which reflects a similar fraction of porphyrin molecules interacting with NEt₃, a similar constitution of both matrices can be assumed. To achieve these properties, an initial porphyrin concentration of 3.00 g L⁻¹ within the precursor solution was necessary for Cr-3, while for CrTPP-1 0.75 g L⁻¹ Cr^{III}TPP(Cl)(H₂O) has been used. Both concentrations represent almost saturated solutions for the respective porphyrin, as the solubility of Cr^{III}P(Cl)(H₂O) in the precursor solution is approximately 5 times higher than the solubility of Cr^{III}TPP(Cl)(H₂O). From diluted solutions as used for the preparation of Cr-1 (0.75 g L⁻¹) and Cr-2 (1.50 g L⁻¹), sensors with lower performance have been obtained. This is seen by their superimposable, but lower, normalized response towards NEt₃ as depicted in Fig. 10a. Accordingly, layers have been

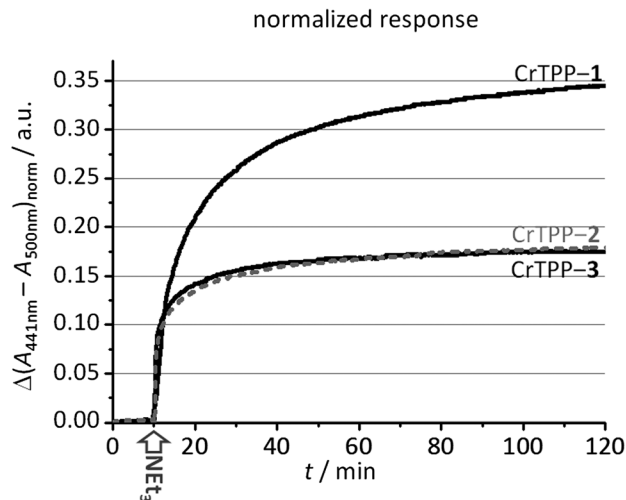


Fig. 11 Time traces for CrTPP-1, CrTPP-2 and CrTPP-3 of the absorption change at 441 nm relative to the absorption at 500 nm upon exposure to a constant gas flow of 1 vol.% NEt₃; data points measured every 10 s; exposure starts at 10 min and response normalized to the initial Soret band intensity.

deposited from diluted Cr^{III}TPP(Cl)(H₂O) precursor solutions containing 0.32 g L⁻¹ and 0.08 g L⁻¹ porphyrin to form CrTPP-2 and CrTPP-3, respectively. As shown in Fig. 11, their optical response towards NEt₃ exposure is also significantly lowered by 52% as compared to CrTPP-1 and is comparable to that observed for Cr-2 and Cr-3. This shows that also in Cr^{III}TPP(Cl)(H₂O) based coatings only a smaller fraction of chromophores interact with the analyte if they are deposited from diluted solutions.

The similar dependence of the sensor responses on the respective initial concentration of Cr^{III}P(Cl)(H₂O) or Cr^{III}TPP(Cl)(H₂O) in the precursor solutions reveals a common influence on the matrix growth mechanism. If the precursor solution's concentration is increased above a certain threshold value, approaching the saturation limit, a matrix/chromophore constitution is achieved which facilitates the interaction of a higher fraction of chromophores with the analyte leading to a remarkably better sensor performance. The detailed mechanism, however, is so far unclear and is under current investigation in our laboratories.

F. Conclusions

Four different metalloporphyrins, Zn^{II}P, Cr^{III}P(Cl)(H₂O), Zn^{II}TPP and Cr^{III}TPP(Cl)(H₂O) were successfully incorporated into porous polysiloxane matrices *via* an atmospheric pressure plasma enhanced chemical vapor deposition. The structure of the metalloporphyrin complexes was entirely stable during the plasma treatment, even the complex molecular structures of Zn^{II}P and Cr^{III}P(Cl)(H₂O) with two phenylalkynyl substituents are fully retained.

Due to the porous nature of the matrix and the amine sensing properties of the incorporated porphyrins, the deposited layers can be used for the colorimetric detection of volatile

amines as exemplified by exposure to NEt_3 . The layers based on zinc porphyrins show a 1 nm bathochromic shift of the Soret band absorption along with a slight increase of intensity upon interaction with NEt_3 . The remarkable color changes observed in *n*-hexane solutions, especially of $\text{Zn}^{\text{II}}\text{P}$, could not completely be transferred to the deposited thin coatings. This behavior is attributed to a solvatochromic effect of the matrix on the porphyrins' absorption properties, as a similar effect is also observed *e.g.* in chloroform solutions.

The Cr^{III} porphyrin containing layers show a larger spectral shift and exhibit a stronger sensor response signal upon interaction with NEt_3 . Layers based on the novel metalloporphyrin $\text{Cr}^{\text{III}}\text{P}(\text{Cl})(\text{H}_2\text{O})$ show a 3 nm hypsochromic shift when exposed to NEt_3 , which is comparable to responses observed for coatings containing $\text{Cr}^{\text{III}}\text{TPP}(\text{Cl})(\text{H}_2\text{O})$. Due to the significantly higher solubility of $\text{Cr}^{\text{III}}\text{P}(\text{Cl})(\text{H}_2\text{O})$ as compared to $\text{Cr}^{\text{III}}\text{TPP}(\text{Cl})(\text{H}_2\text{O})$, coatings with higher chromophore loading could be produced. This leads to a visible intense coloration of the foils and a stronger response upon NEt_3 exposure. The 3 nm shift of the Soret band may only be seen by a trained eye without any support. Nevertheless, the absorbance change can easily be monitored spectroscopically fully similar to existing amine sensors. The signal-to-noise ratio is greatly enhanced up to 117.6 which is beneficial for the production of amine sensing devices.

Higher porphyrin loadings not only proportionally increase the coloration and the sensitivity of the sensor, but also a certain non-linear effect is noted. Above a certain threshold concentration the constitution of the deposited matrices is changed in such a way that a higher fraction of chromophores interacts with the analyte. This leads to an improvement of the normalized sensor response of 140% for $\text{Cr}^{\text{III}}\text{P}(\text{Cl})(\text{H}_2\text{O})$ based coatings and 200% for $\text{Cr}^{\text{III}}\text{TPP}(\text{Cl})(\text{H}_2\text{O})$ based ones.

As functionalized porphyrins have been deposited unaltered *via* an atmospheric pressure plasma enhanced CVD for the first time, new possibilities to improve the sensing layer properties open up. The possibility to use further optimized porphyrins or other chromophore classes may finally lead to colorimetric sensing foils which (i) show a visible color change and (ii) have been produced by this environmentally friendly and easy to scale up process. The potential demonstrated here may be inspiring for researchers working in the fields of hybrid functional materials and immobilization of organic compounds in general.

Acknowledgements

The authors thank the Luxembourgish "Fonds National de la Recherche" (FNR) for financial support through the SurfAmine CORE project. Skillful characterizations of and valuable discussions with Dr C. Guignard, Dr G. Frache and J. Didierjean from the CRP-Gabriel Lippmann are gratefully acknowledged.

References

1 L.-L. Li and E. W.-G. Diau, *Chem. Soc. Rev.*, 2013, **42**, 291.

- 2 A. Yella, H.-W. Lee, H. N. Tsao, C. Yi, A. K. Chandiran, M. K. Nazeeruddin, E. W.-G. Diau, C.-Y. Yeh, S. M. Zakeeruddin and M. Grätzel, *Science*, 2011, **334**, 629.
- 3 H. Imahori, S. Kang, H. Hayashi, M. Haruta, H. Kurata, S. Isoda, S. E. Canton, Y. Infahsaeng, A. Kathiravan, T. Pascher, P. Chábera, A. P. Yartsev and V. Sundström, *J. Phys. Chem. A*, 2011, **115**, 3679.
- 4 A. Huijser, T. J. Savenije, A. Kotlewski, S. J. Picken and L. D. A. Siebbeles, *Adv. Mater.*, 2006, **18**, 2234.
- 5 C.-L. Wang, W.-B. Zhang, R. M. Van Horn, Y. Tu, X. Gong, S. Z. D. Cheng, Y. Sun, M. Tong, J. Seo, B. B. Y. Hsu and A. J. Heeger, *Adv. Mater.*, 2011, **23**, 2951.
- 6 Z. Liu, A. a. Yasseri, J. S. Lindsey and D. F. Bocian, *Science*, 2003, **302**, 1543.
- 7 M. O. Senge, M. Fazekas, E. G. A. Notaras, W. J. Blau, M. Zawadzka, O. B. Locos and E. M. N. Mhuirheartaigh, *Adv. Mater.*, 2007, **19**, 2737.
- 8 M. H. Hoang, Y. Kim, M. Kim, K. H. Kim, T. W. Lee, D. N. Nguyen, S.-J. Kim, K. Lee, S. J. Lee and D. H. Choi, *Adv. Mater.*, 2012, **24**, 5363.
- 9 S.-J. Choi, Y.-C. Lee, M.-L. Seol, J.-H. Ahn, S. Kim, D.-I. Moon, J.-W. Han, S. Mann, J.-W. Yang and Y.-K. Choi, *Adv. Mater.*, 2011, **23**, 3979.
- 10 A. Huijser, B. M. J. M. Suijkerbuijk, R. J. M. Klein Gebbink, T. J. Savenije and L. D. A. Siebbeles, *J. Am. Chem. Soc.*, 2008, **130**, 2485.
- 11 B. Johnson-White, M. Zeinali, K. M. Shaffer, C. H. Patterson Jr, P. T. Charles and M. A. Markowitz, *Biosens. Bioelectron.*, 2007, **22**, 1154.
- 12 S. Tao, G. Li and H. Zhu, *J. Mater. Chem.*, 2006, **16**, 4521.
- 13 M. Tonezzer, G. Maggioni and E. Dalcanale, *J. Mater. Chem.*, 2012, **22**, 5647.
- 14 T. H. Richardson, R. A. Brook, F. Davis and C. A. Hunter, *Colloids Surf., A*, 2006, **284–285**, 320.
- 15 O. Worsfold, C. M. Dooling, T. H. Richardson, M. O. Vysotsky, R. Tregonning, C. A. Hunter and C. Malins, *Colloids Surf., A*, 2002, **200**, 859.
- 16 N. A. Rakow and K. S. Suslick, *Nature*, 2000, **406**, 710.
- 17 A. D. F. Dunbar, S. Brittle, T. H. Richardson, J. Hutchinson, C. A. Hunter, D. Building, B. Hill and S. Sheffield, *J. Phys. Chem. B*, 2010, 11697.
- 18 S. a. Brittle, T. H. Richardson, A. D. F. Dunbar, S. M. Turega and C. a. Hunter, *J. Mater. Chem.*, 2011, **21**, 4882.
- 19 C. Di Natale, D. Salimbeni, R. Paolesse, A. Macagnano and A. D'Amico, *Sens. Actuators, B*, 2000, **65**, 220.
- 20 S. H. Lim, L. Feng, J. W. Kemling, C. J. Musto and K. S. Suslick, *Nat. Chem.*, 2009, **1**, 562.
- 21 M. Tonezzer, G. Maggioni, A. Quaranta, S. Carturan and G. Della Mea, *Sens. Actuators, B*, 2009, **136**, 290.
- 22 M. Tonezzer, A. Quaranta, G. Maggioni, S. Carturan and G. Della Mea, *Sens. Actuators, B*, 2007, **122**, 620.
- 23 S. Kladsomboon and T. Kerdcharoen, *Anal. Chim. Acta*, 2012, **757**, 75.
- 24 D. Delmarre and C. Bied-Charreton, *Sens. Actuators, B*, 2000, **62**, 136.
- 25 W. Qin, P. Parzuchowski, W. Zhang and M. E. Meyerhoff, *Anal. Chem.*, 2003, **75**, 332.

- 26 J. Spadavecchia, R. Rella, P. Siciliano, M. G. Manera and A. Alimelli, *Sens. Actuators, B*, 2006, **115**, 12.
- 27 F. A. Nwachukwu and M. G. Baron, *Sens. Actuators, B*, 2003, **90**, 276.
- 28 N. A. Rakow, A. Sen, M. C. Janzen, J. B. Ponder and K. S. Suslick, *Angew. Chem., Int. Ed.*, 2005, **44**, 4528.
- 29 M. T. Veciana-Nogués, A. Mariné-Font and M. C. Vidal-Carou, *J. Agric. Food Chem.*, 1997, **45**, 2036.
- 30 C. Balamatsia, A. Patsias, M. Kontominas and I. Savvaidis, *Food Chem.*, 2007, **104**, 1622.
- 31 Y. Xu, W. Xia and J. M. Kim, *Int. J. Food Sci. Technol.*, 2009, **44**, 1547.
- 32 J. P. Kerry, M. N. O'Grady and S. A. Hogan, *Meat Sci.*, 2006, **74**, 113.
- 33 T. H. Richardson, C. M. Dooling, L. T. Jones and R. A. Brook, *Adv. Colloid Interface Sci.*, 2005, **116**, 81.
- 34 C. M. Dooling, O. Worsfold, T. H. Richardson, R. Tregonning, M. O. Vysotsky, C. A. Hunter, K. Kato, K. Shinbo and F. Kaneko, *J. Mater. Chem.*, 2001, **11**, 392.
- 35 A. D. F. Dunbar, T. H. Richardson, J. Hutchinson and C. A. Hunter, *Sens. Actuators, B*, 2008, **128**, 468.
- 36 A. A. Vaughan, M. G. Baron and R. Narayanaswamy, *Anal. Commun.*, 1996, **33**, 393.
- 37 P. Heyse, R. Dams, S. Paulussen, K. Houthoofd, K. Janssen, P. a. Jacobs and B. F. Sels, *Plasma Processes Polym.*, 2007, **4**, 145.
- 38 C. Tendero, C. Tixier, P. Tristant, J. Desmaison and P. Leprince, *Spectrochim. Acta, Part B*, 2006, **61**, 2.
- 39 R. Prat, Y. Koh, Y. Babukutty, M. Kogoma, S. Okazaki and M. Kodama, *Polymer*, 2000, **41**, 7355.
- 40 N. D. Boscher, P. Choquet, D. Duday and S. Verdier, *Plasma Processes Polym.*, 2010, **7**, 163.
- 41 N. D. Boscher, P. Choquet, D. Duday and S. Verdier, *Surf. Coat. Technol.*, 2011, **205**, 5350.
- 42 U. Kogelschatz, *Plasma Chem. Plasma Process.*, 2003, **23**, 1.
- 43 N. D. Boscher, P. Choquet, D. Duday, N. Kerbellec, J.-C. Lambrechts and R. R. Maurau, *J. Mater. Chem.*, 2011, **21**, 18959.
- 44 J. Bardon, J. Bour, D. Del Frari, C. Arnoult and D. Ruch, *Plasma Processes Polym.*, 2009, **6**, S655.
- 45 P. Heyse, A. Van Hoeck, M. B. J. Roefsaers, J.-P. Raffin, A. Steinbüchel, T. Stöveken, J. Lammertyn, P. Verboven, P. A. Jacobs, J. Hofkens, S. Paulussen and B. F. Sels, *Plasma Processes Polym.*, 2011, **8**, 965.
- 46 N. D. Boscher, D. Duday, P. Heier, K. Heinze, F. Hilt and P. Choquet, *Surf. Coat. Technol.*, 2013, **234**, 48.
- 47 N. D. Boscher, D. Duday, P. Heier, K. Heinze, F. Hilt and P. Choquet, *Plasma Processes Polym.*, 2013, **10**, 336.
- 48 N. D. Boscher, T. Bohn, P. Heier, F. Moisy, B. Untereiner, K. Heinze and P. Choquet, *Sens. Actuators, B*, 2014, **191**, 553.
- 49 P. Heier, C. Förster, D. Schollmeyer, N. Boscher, P. Choquet and K. Heinze, *Dalton Trans.*, 2013, **42**, 906.
- 50 D. A. Summerville, R. D. Jones, B. M. Hoffmann and F. Basolo, *J. Am. Chem. Soc.*, 1977, **99**, 8195.
- 51 N. D. Boscher, P. Choquet, D. Duday and S. Verdier, *Surf. Coat. Technol.*, 2010, **205**, 2438.
- 52 M. Gouterman, L. K. Hanson, G.-E. Khalil, W. R. Lenstra and J. W. Buchler, *J. Chem. Phys.*, 1975, **62**, 2343.